J. Pestic. Sci. **45**(3), 151–158 (2020)
DOI: 10.1584/jpestics.J20-04

Society Awards 2020
(on high prospectiveness)

Study of uptake, translocation, and metabolic behavior of pesticides in water milfoil

Daisuke Ando*

Environmental Health Science Laboratory, Sumitomo Chemical Co., Ltd., 4–2–1 Takarazuka, Hyogo 665–8555, Japan

(Accepted July 2, 2020)

Water milfoil is a sediment-rooted macrophyte contributing to the aquatic ecosystem, and the risk evaluation of pesticides on this new assessment species has attracted much attention. Knowledge of the shoot/root uptake, inner-plant translocation, and the metabolism of pesticides in water milfoil is essential for a detailed risk assessment and understanding toxicological mechanisms thereof; however, the behaviors have not been studied in detail. Using model studies, the author clarified shoot and root uptake dynamics of 3-phenoxybenzoic acid *via* water and sediment exposure, respectively, followed by transportation and metabolism at each plant portion; uptake and metabolism kinetics of simple phenols amended with regression analysis on physico-chemical parameters of the compounds; detailed metabolic fate of flumioxazin in various aquatic plants/phytoplankton, and an interspecies comparison. Similar approaches are fully applicable to clarifying the fate of pesticides in water milfoil and are expected to be useful for implementing advanced risk characterizations.

Keywords: water milfoil, pesticide metabolism, shoot uptake, root uptake, translocation.

Introduction

Synthetic pesticides efficiently contribute to stable agricultural crop yield and supply by controlling harmful target insects, fungi, and weeds. While providing benefits, the chemicals may cause adverse effects for humans and wildlife *via* crop consumption and unintended exposure. Likewise, freshwater aquatic organisms can potentially be exposed to pesticides through unintentional contamination by spray drift, run-off, drainage, or accidental spills during and after agricultural usage; hence, evaluation of aquatic biota risk is indispensable. The freshwater aquatic ecosystem consists of diverse organisms—including aquatic plants, plankton, larger fish, and other predators—through complex biological interactions therein. In the aquatic ecology, aquatic plants and phytoplankton are serving as primer producers vital for oxygen circulation, carbon fixation, nutrient nourishment and trapping/resuspension of other trace elements; they directly influence the hydrology and sediment dynamics of securing food and supplying shelter for aquatic lives.[1–5] Due to their specific mode of actions designed for plants, herbicides and plant-growth regulators could directly cause substantial damage to aquatic flora (and often phytoplankton); the impact could even be expanded to degrading the balance of the entire aquatic ecosystem. For these reasons, evaluating the risk for aquatic plants has gained much attention.

In the previous risk assessment on aquatic plants/phytoplankton, duckweed and algae were the major test species toxicologically evaluated to determine fundamental adverse effects on freshwater aquatic plants/phytoplankton in Japan and other countries. However, in the EU, assessment with these floating and suspended species only had been considered limited and insufficient to cover the overall aquatic flora/phytoplankton. Particularly, by focusing on the potential of sediment-rooted macrophytes, which contribute to sediment acclimatization, chemical uptake not only from the water column but additionally from the bottom sediment *via* roots (Fig. 1), and the possibility that species express unequal sensitivity as compared with the original test organisms,[5–8] in 2013, water milfoil was included as an additional species for toxicity testing.[9]

Currently, the accumulation of pesticide toxicological data, *e.g.*, EC_{50} and NOEC, on water milfoil has progressed to the point being useful, whereas, information on the metabolic behavior of the species when exposed to the compound is still not sufficiently available. Notably, metabolism research combined with quantitative analysis of shoot/root uptake followed by

* To whom correspondence should be addressed.
E-mail: andod@sc.sumitomo-chem.co.jp
Published online July 22, 2020

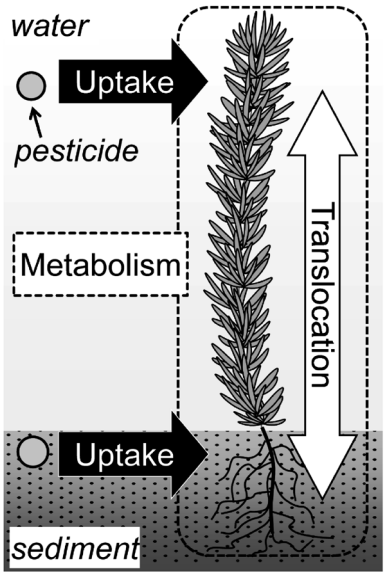

Fig. 1. Schematic dynamics of a pesticide on water milfoil in aquatic environment.

translocation has been very limited. Such detailed knowledge of individual dynamics, metabolism, and distribution of the product in the macrophyte is essential for a detailed risk evaluation and for understanding the toxicological mechanism. Moreover, the residue pattern of pesticide-derived molecules in the macrophyte is useful for discussing biomagnification and adverse effects on higher organisms/predators through the trophic food chain. From such a respective, the author has studied the dynamics and metabolic behavior of xenobiotics in water milfoil. In this article, the following results are summarized: the development of a sequestered chamber able to separately expose shoot and roots, and the individual quantification of shoot/root uptake dynamics, followed by translocation and metabolism of a model compound 3-phenoxybenzoic acid; a kinetic analysis of uptake and metabolic behaviors of simple phenols with regression analysis on physico-chemical properties; detailing the metabolic behavior of flumioxazin in various aquatic plants/phytoplankton and comparing their metabolic profiles.

1. Development of a Sequestered Exposure Chamber: Clarification of Shoot/Root Uptake, Translocation, and Metabolism

In the natural freshwater environment, water milfoil uptake a pesticide through two major routes, namely, shoot exposure *via* a water column and root exposure *via* bottom sediment (Fig. 1). Following each uptake, the pesticide is expected to be translocated at inner tissues from shoot to root and *vice versa* while receiving metabolization/detoxification; since these are simultaneous events, the overall dynamics of the pesticide in water milfoil are expected to be complicated. To understand each dynamic, it is imperative to separately expose the shoot and roots to the pesticide; however, the previous exposure systems, applied to a separate water column and sediment regions, were considered insufficient due to the possible direct exchange of the test substance between the layers through artificial gaps and the adsorption of the substance to the partitioning material.[10,11] Hence, the author designed a new exposure chamber with a partition glass board (Fig. 2) by modifying the exposure system used by Fritioff *et al.*[12] Using the sequestered chamber, the behavior in water milfoil of 3-phenoxybenzoic acid (PBA), uniformly ^{14}C-radiolabeled at the β-phenoxyphenyl ring, was investigated as a model study.[13]

The autoclaved American Academy of Pediatrics (AAP) water medium[14] and AAP-moistened Organisation for Economic Co-operation and Development (OECD) sediment[15] adjusted to pH 7.0±0.5 were filled into each side of the chamber. Either the medium or the sediment was treated with [^{14}C]-PBA at an exposure concentration of 3.3 ppm by sufficiently accounting for the radioactivity detection limit. The shoot and root portions of *Myriophyllum elatinoides* (length: 16.5–18.3 cm; fresh body weight: 0.34–0.51 g), sterilized using 0.5% sodium hypochlorite with sonication under reduced pressure, were immersed and buried (*ca.* 1.5 cm of the root tips) in the corresponding compartment. The chamber was wrapped with a polyethylene sheet and incubated in a climate chamber at 20±2°C (16 hr light per day) for up to 14 days. The radioactivity and the ^{14}C constituents in each chamber were sequentially analyzed, while the plant was divided into shoot and root portions and individually processed.

No growth inhibition of *M. elatinoides* in the exposure chamber was confirmed when comparing the increase of length (1.1–1.8 cm) and fresh weight (0.7–0.11 g) with those of the plant vertically grown in an aquarium filled with the water medium and sediment without exposure. No radioactivity was detected in the untreated chamber for both water and sediment exposures, demonstrating that there was no ^{14}C cross-contamination between the chambers and excretion from the plant.

In the water treatment, more than 96.5%AR (AR: applied radioactivity) was recovered from the water medium and the plant. All of the ^{14}C remained in the medium was the unchanged PBA throughout the incubation period. After the exposure, the radioactivity in the medium was rapidly incorporated into

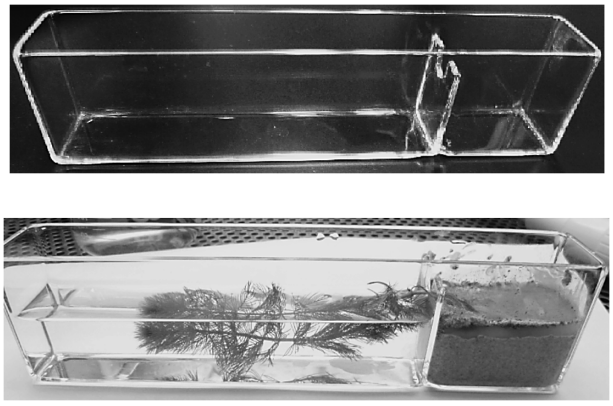

Fig. 2. Designed sequestered chamber to separately expose water and sediment layers.

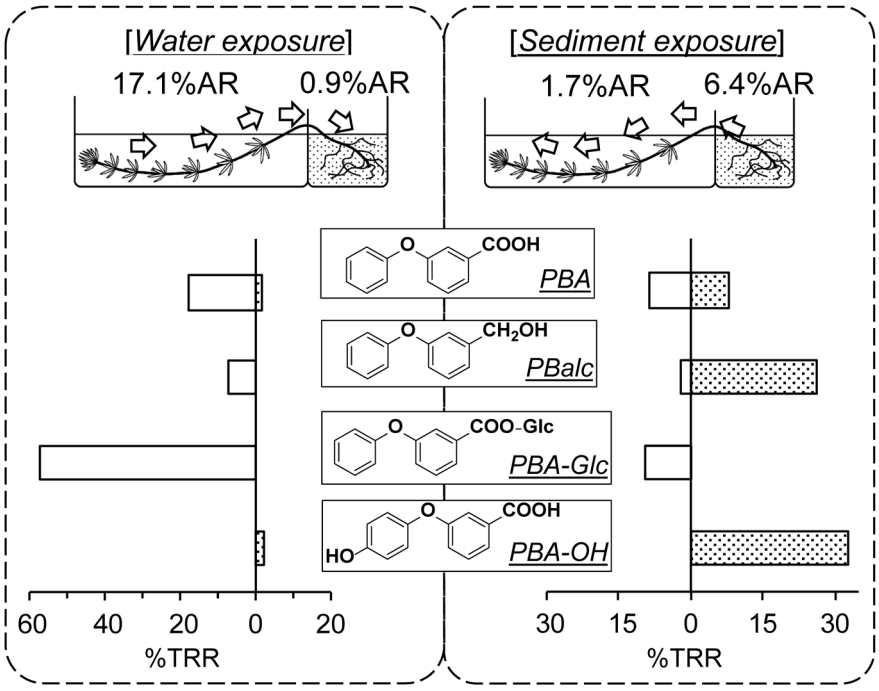

Fig. 3. Distribution of 3-phenoxybenzoic acid (PBA) and its metabolites in shoot and root portions exposed *via* water (left) or sediment (right) layer. White and stippled bars correspond to the shoot and root portions, respectively.

the shoot, likely reaching the uptake plateau on Day 0.5. The total ^{14}C accumulated in the shoot accounted for 18.0%AR after 14 days, whereas the amount in the roots was much lower as 0.9%AR, indicated that basipetal translocation was a minor process (Fig. 3). The major ^{14}C molecules identified in the shoot on Day 14, which were characterized by LC-MS and NMR analyses, were PBA, the reduction product (PBalc), and the glucose ester conjugate of PBA (PBA-Glc), amounting to 17.8, 7.0, and 57.1%TRR (TRR: total radioactive residues in the plant), respectively. In the roots, PBA and the hydroxylated product at the 4′ position of the β-phenoxyphenyl ring (PBA-OH) were detected at 1.8 and 2.3%TRR, respectively. The other minor metabolites and the unextractable residues in the whole plant were 5.0 and 9.1%TRR, respectively.

In case of the sediment treatment, AR greater than 87.2% was detected from the root chamber and plant, most of which was distributed in the interstitial medium water of the sediment, *i.e.*, pore water, ≥78.6%AR. The only radioactive component in the pore water and sediment fractions was elucidated as PBA. The radioactivity applied in the sediment was gradually taken up by the roots, which reached the maximum of 8.1%AR after 14 days. In the water milfoil, the majority of accumulated ^{14}C was located in the roots (6.4%AR). However, in contrast to the case of water exposure, 1.7%AR (equivalent to *ca.* 1/4 of the total radioactivity taken up) was detected in the shoot portion, suggesting the significance of acropetal transportation. The radioactive constituents in the ^{14}C-exposed roots were PBA, PBalc, and PBA-OH, accounting for 8.0, 26.1, and 32.4%TRR, respectively. In the shoot, PBA (8.6%TRR), PBalc (2.0%TRR), and PBA-Glc (9.4%TRR) were detected. The other minor components and the unextractable radioactivities in whole plant were 0.9 and 8.0%TRR, respectively.

In summary, to distinguish the contribution of each shoot and root uptake, a new exposure chamber was designed. Using the system, each dynamic regarding uptake, acropetal/basipetal translocation, and metabolism of PBA in shoot and root portions through water and sediment exposures was individually clarified/quantitated for the first time. While the identified metabolites of PBA in water milfoil were mostly the same as those reported for terrestrial plants[16] and duckweed,[17] shoot- and root-specific metabolic reactions, which probably resulted from differences in enzyme distribution,[18] were successfully distinguished.

2. Kinetic Analysis of Uptake and Metabolism

Using the developed exposure system, the behaviors of phenol (**1**), 4-nitrophenol (**2**), 4-cyanophenol (**3**), 4-hydroxybenzamide (**4**), and 4-hydroxybenzoic acid (**5**) in water milfoil were examined.[19] The kinetics of uptake and metabolic reactions by the plant were determined and compared with various physicochemical parameters of the test phenols. Exposure experiments similar to those of the previous model study[13] were performed with an exposure concentration of 0.1 ppm and an incubation period of 96 hr. The kinetics analysis of the water-exposed macrophyte was performed using the Model Maker program while applying a compartment model, as shown in Fig. 4. The fraction of the undissociated form of each phenol in the medium at pH 7 was calculated from its acid dissociation constant (K_a)

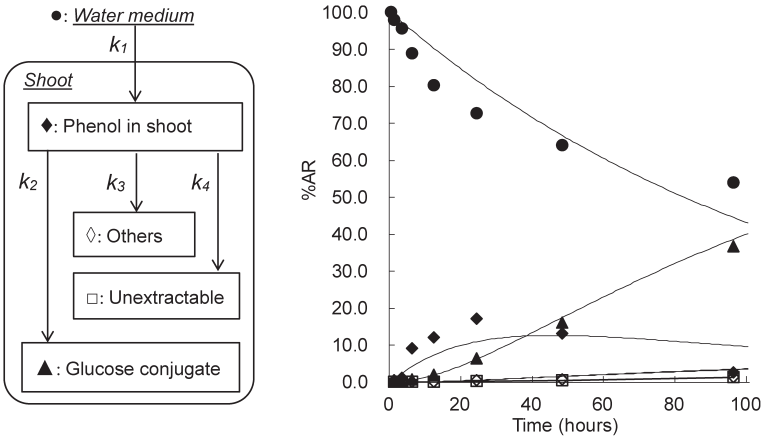

Fig. 4. Compartment model for kinetics simulation (left) and the representative ^{14}C transition curve of 4-hydroxybenzoic acid (**5**) (right).

by the Henderson–Hasselbalch equation. The logarithm of the distribution coefficient (log *D*), which indicates the hydrophobicity of chemicals adjusted with their dissociation effects, was obtained from the log K_{ow} and pK_a values according to the reported calculation method.[20] The highest occupied molecular orbital energy (E_{HOMO}, eV) of each phenol was calculated as a nucleophilic reaction potential index by SCIGRESS MO Compact program with MNDO-PM-3 Hamiltonian introducing the dielectric constant of ε=78.4 to assume the water environment. The calculation was conducted for the neutral and ionized forms abbreviated as $E_{HOMO(OH)}$ and $E_{HOMO(O^-)}$, respectively. The classical Hammett's constants (σ and σ^-) at the reaction center, *i.e.*, phenolic oxygen, were also examined.[21]

In the water treatment system, the total ^{14}C recovery for **2**–**5** ranged from 93.7–97.2%AR at the end of the exposure, with a lower ratio for **1** (81.3%AR) due to volatilization. A large amount of AR remained in the water for **2**–**4** (>80.9%AR), while a lower level was observed for **1** (55.8%AR) and **5** (54.5%AR). Shoot uptake gradually occurred, approaching its steady state, which reached 25.5, 14.3, 12.8, 4.2, and 41.7%AR for **1**, **2**, **3**, **4**, and **5**, respectively, after 96 hr. The majority of the ^{14}C taken up remained in the shoot, and minor radioactivity was detected from the root portion, which accounted for 0.4% (**1**), ≤0.1% (**2**–**4**) and 0.9%AR (**5**). In the plant, the unchanged phenols were quantified to be 14.0–20.5%TRR for **1**–**4**, while the one for **5** was only 6.0%TRR (Table 1). The glycoside conjugate at the phenoxy oxygen, confirmed by LC-MS and NMR analyses, was the main metabolite for all of the test substances, which amounted to 63.5–88.0%TRR. The other minor metabolites and unextractable ^{14}C were 0.6–10.8% and 2.5–6.3%TRR, respectively. The ^{14}C residues in the roots were not analyzed due to their low radioactivities.

With respect to the sediment treatment, the total ^{14}C recovery ranged from 91.7–98.2%AR throughout the exposure. The ^{14}C distributions at the pore water/sediment in the root chamber after 96 hr were 47.0/42.1 (**1**), 34.4/61.0 (**2**), 42.2/51.8 (**3**), 85.9/11.5 (**4**), and 84.3%AR/6.5%AR (**5**). The unextractable residues in sediment were determined to be less than 3.5%AR. The ^{14}C root uptake moderately proceeded to reach 0.8–2.4%AR for **1**–**4** and 6.6%AR for **5** after 96 hr. The radioactivity translocated from root to shoot after 96 hr was extremely low for **1**–**4** (≤0.1%AR), while **5** showed the highest transportation potential (1.5%AR). Due to their low ^{14}C residue levels, the radioactive components in roots and shoots were uncharacterized.

A kinetic analysis was conducted for the water treatment system. The simulated ^{14}C-dissipation curves of **5**, as representative, are given in Fig. 4. The rate constants were optimized with a good correlation (r^2 >0.97, p<0.05). The relative rate constants

Table 1. ^{14}C metabolites in shoot exposed for 96 hr in the water treatment system

	%TRR[a]				
	1	**2**	**3**	**4**	**5**
Extractable					
Phenols	20.5 (2.9)	17.9 (1.9)	14.0 (1.6)	19.4 (2.0)	6.0 (0.7)
Glucose conjugate	72.9 (7.3)	78.8 (7.7)	83.4 (8.1)	63.5 (5.9)	88.0 (8.1)
Others[b]	0.8 (0.1)	0.6 (0.1)	<0.1	10.8 (1.0)	2.9 (0.2)
Unextractable	5.8 (0.6)	2.7 (0.3)	2.5 (0.2)	6.3 (0.5)	3.1 (0.2)
Total	100.0	100.0	100.0	100.0	100.0

[a] Average values (n=3). Standard deviations are given in parentheses. [b] Minor degradates amounted less than 5%TRR and/or polar degradates un-retained by the HPLC column.

Table 2. Kinetic obtained for **1**–**5** in water milfoil (water exposure system)

	1	**2**	**3**	**4**	**5**
Rate constant (hrs^{-1})					
k_1 (uptake)	5.651×10^{-3}	2.332×10^{-3}	2.818×10^{-3}	9.063×10^{-4}	8.424×10^{-3}
k_2 (conjugation)	3.185×10^{-2}	4.359×10^{-2}	4.044×10^{-2}	4.193×10^{-2}	3.851×10^{-2}
k_3 (others)	6.389×10^{-3}	9.574×10^{-4}	6.346×10^{-3}	1.815×10^{-2}	3.323×10^{-3}
k_4 (unextractable)	8.284×10^{-3}	2.067×10^{-3}	1.064×10^{-2}	1.741×10^{-2}	3.489×10^{-3}
r^2	0.997	0.989	0.990	0.978	0.989
p	3.210×10^{-3}	1.866×10^{-2}	3.731×10^{-4}	4.209×10^{-2}	2.677×10^{-6}
Relative rate constant					
$\log [k_{1(i)}/k_{1(1)}]$	0	−0.384	−0.302	−0.795	0.173
$\log [k_{2(i)}/k_{2(1)}]$	0	0.136	0.104	0.119	0.083

of **2**–**5** against **1** are summarized in Table 2. Successively, the correlations between the physicochemical parameters and the logarithm of the relative rate constants were examined by regression analysis for shoot uptake and glucose conjugation (Table 3). The constants of "others" and "unextractable" were not examined due to their insignificant contribution to the overall metabolic processes. The highest positive correlation for shoot uptake (k_1) was observed for log K_{ow} as |0.656| (standard deviation: 0.325), which was similar to the trend observed for other sediment-rooted macrophytes on non-dissociable compounds.[22–24] The second-highest negative correlation obtained for $f_{neutral}$ supports the importance of the hydrophobicity of chemicals in the accumulation. The log D constant was another candidate, as it was reported to have better positive correlation than log K_{ow} for the accumulation of ionized chemicals by fish.[25] However, a poor correlation was obtained in our study, especially due to the fact that extensively ionized **5** exhibited the highest accumulation in contrast to the lowest log D value. Likewise, it was reported that many weak acid compounds were highly bioaccumulated in spite of their relatively low lipophilicity by macrophytes in water.[13,26] As such, chemicals with moderate acidic function likely have high accumulative potential, which can probably be explained by enhanced deprotonation followed by efficient trapping at slightly alkaline inner tissues or cells (ion trap theory).[27] With respect to the transformation rate to glucose conjugate (k_2), good correlations (≥|0.807|, standard deviation <0.036) were obtained for σ, σ^-, and $E_{HOMO(OH)}$. These results suggest that the electronic distribution and nucleophilicity at the phenoxy group through the inductive effect of the electron-withdrawing substituent are important for the glucosidation reaction at the active site of glycosyltransferase. While good correlations were confirmed to provide basic relationships, further detailed simulations—such as the introduction of the orbital energy gap between the nucleophile (aglycone) and electron acceptor and/or the transition state through interaction with the binding/catalytic amino acid residues at the reaction pocket followed by electron/orbital re-distribution—are expected to be important for more precise analysis.[28,29]

3. Metabolism Comparison of Flumioxazin Among Various Aquatic Plants/Phytoplankton

The metabolic fate of the herbicide flumioxazin (**I**), radiolabeled at the carbonyl carbons of the tetrahydrophthaloyl moiety (abbreviated as [THP-^{14}C]) or at the phenyl ring ([PH-^{14}C]), in two algae (*Pseudokirchneriella subcapitata* and *Synechococcus* sp.), duckweed (*Lemna* sp.), and water milfoil was examined to compare their metabolic potential.[30] Each organism was exposed to [^{14}C]**I** *via* water treatment at a concentration of 0.020 ppb, based on the predicted environmental concentration of surface water (PEC_{sw}) in EU ponds simulated using FOCUSsw step 3 program[31] by inputting the intended agricultural use scenario and various physico-chemical and environmental fate parameters of the herbicide. Each alga at the exponential growth stage and each *Lemna* sp. with 3–5 fronds were subjected to the water exposure experiment. With respect to water milfoil, the water and sediment (0.020 ppb on wet sediment basis) treatments were conducted separately using the sequestered chamber. The exposure duration was 14 days for all test systems.

In the water exposure system, the [^{14}C]**I** rapidly decomposed to **II** (maleimide ring-opened product) in the water and reached the maximum of 82.0%AR after 3 days. In parallel, continuous increase of **IV** (3,4,5,6-tetrahydrophthalic acid) and **V** (the counterpart of **IV**) was observed in the water throughout the incubation period for [THP-^{14}C] and [PH-^{14}C], which reached 45.2–54.2 and 18.5–27.5%AR after 14 days, respectively (Table 4). For both radiolabels, **III** (ring-modified product) was de-

Table 3. Correlation between the relative rate constant and physico-chemical parameters of the phenols for shoot uptake and glucose conjugation

	pK_a	$f_{neutral}$	log K_{ow}	log D	σ	σ^-	$E_{HOMO(OH)}$	$E_{HOMO(O^-)}$
$\log [k_{1(i)}/k_{1(1)}]$	−0.323	−0.564	0.656	−0.159	−0.263	−0.261	0.178	0.546
$\log [k_{2(i)}/k_{2(1)}]$	−0.467	−0.208	−0.100	−0.033	0.872	0.890	−0.807	−0.265

Table 4. ^{14}C distribution in the water exposure system after 14 days[a)]

	%AR[b)]							
	[THP-^{14}C]				[PH-^{14}C]			
	P. subcapitata	*Synenocossus*	*Lemna* sp.	*M. elatinoides*	*P. subcapitata*	*Synenocossus*	*Lemna* sp.	*M. elatinoides*
Water layer	97.1 (1.9)	97.7 (1.8)	97.3 (0.6)	95.3 (0.7)	95.0 (1.9)	95.5 (2.6)	91.6 (0.8)	95.0 (1.0)
I	0.1 (<0.1)	0.1 (<0.1)	3.2 (1.9)	1.0 (0.3)	ND	ND	0.1 (<0.1)	0.1 (<0.1)
II	44.5 (3.2)	43.2 (4.1)	40.2 (3.6)	48.2 (3.6)	51.9 (3.4)	58.3 (4.0)	59.2 (3.6)	52.7 (3.6)
III	0.2 (0.1)	ND	0.4 (0.2)	0.6 (0.3)	ND	ND	0.3 (0.2)	0.3 (0.2)
IV	50.2 (3.5)	54.2 (4.8)	50.3 (3.5)	45.2 (4.2)	NA	NA	NA	NA
V	NA	NA	NA	NA	23.9 (4.1)	18.5 (3.3)	20.8 (3.7)	27.5 (3.5)
Others[c)]	2.1 (0.8)	0.2 (0.1)	3.2 (1.1)	0.3 (0.1)	19.2 (4.7)	18.7 (4.9)	11.2 (4.0)	14.5 (4.3)
Plant/plankton	2.0 (0.6)	2.1 (1.1)	1.9 (0.5)	3.5 (0.3)	3.0 (1.5)	4.0 (1.9)	3.5 (0.4)	4.7 (0.4)
I[d)]	0.1	ND	0.1	0.1	ND	0.1	0.1	ND
II[d)]	0.4	0.3	0.5	0.7	0.3	0.7	0.9	0.9
III[d)]	ND	ND	ND	ND	ND	ND	ND	ND
IV[d)]	1.0	0.9	0.7	1.5	NA	NA	NA	NA
V[d)]	NA	NA	NA	NA	0.6	0.7	0.5	0.7
V-MA[d)]	NA	NA	NA	NA	0.1	ND	0.2	0.3
V-LA[d)]	NA	NA	NA	NA	ND	ND	<0.1	0.2
V-Ac[d)]	NA	NA	NA	NA	0.1	0.1	0.2	0.3
VI[d)]	<0.1	0.2	0.1	0.3	NA	NA	NA	NA
VI-Glc[d)]	0.2	0.3	0.3	0.6	NA	NA	NA	NA
Others[d,e)]	0.3	0.3	0.1	0.1	1.4	1.9	1.2	1.6
Bound[d)]	<0.1	0.1	0.1	0.2	0.5	0.5	0.4	0.7
Total	99.1 (1.7)	99.8 (1.9)	99.2 (0.6)	98.8 (0.9)	98.0 (2.0)	99.5 (2.7)	95.1 (0.6)	99.7 (1.2)

[a)] ND: Not detected, NA: not applicable. [b)] Average values (n=3). Standard deviations are given in parentheses. [c)] Multiple components ([THP-^{14}C] <2.0%AR and [PH-^{14}C] <4.3%AR, each). [d)] Triplicates samples were mixed before HPLC or combustion analysis. [e)] Multiple components ([THP-^{14}C] <0.2%AR and [PH-^{14}C] <0.3%AR, each).

tected as an ephemeral product not exceeding 1.0%AR. Other degradates accounted for the total maximum of 1.2 (Day 10) and 17.1%AR (Day 14, <5%AR as single) for [THP-^{14}C] and [PH-^{14}C], respectively. Such time-dependent ^{14}C distribution in the water, as shown in Fig. 5 for the water milfoil system, was similar for all water exposure systems with and without test species. The ^{14}C uptake gradually plateaued toward the end of the exposure period, approaching a steady state for each test species (Fig. 6). The %AR and **I**-based concentration per organism wet weight (ppb) at the end of the exposure were calculated to be: %AR (ppb), 2.0–3.0 (0.168–0.358), 2.1–4.0 (0.216–0.575), 1.9–3.5 (0.097–0.158), and 3.5–4.7 (0.187–0.221) for *P. subcapitata*, *Synechococcus* sp., *Lemna* sp., and *M. elatinoides*, respectively. In the root portion of the water milfoil, there was no detectable radioactivity. In the test species, unaltered **I** was minor (≤0.1%AR). The major constituents for [THP-^{14}C] were **II** and **IV**, which amounted to 0.3–0.7 and 0.7–1.5%AR, respectively. The mono-hydroxylate of **IV** (**VI**) and its glucose conjugate (**IV**-Glc), characterized by LC-HRMS analysis, were detected at the maximum of 0.3 and 0.6%AR, respectively. In the [PH-^{14}C] label, **II** and **V** accounted for 0.3–0.9 and 0.5–0.7%AR , respectively. Three conjugates of **V**, namely, malonic acid (**V**-MA), lactic acid (**V**-LA), and acetyl (**V**-Ac) conjugates, each assigned by LC-HRMS, accounted for the maximum values of 0.3, 0.2, and 0.3%AR, respectively, while the distribution of these metabolites was somewhat dependent on the test species. In the sediment exposure additionally examined for *M. elatinoides*, the applied radioactivity gradually distributed from the pore water to the

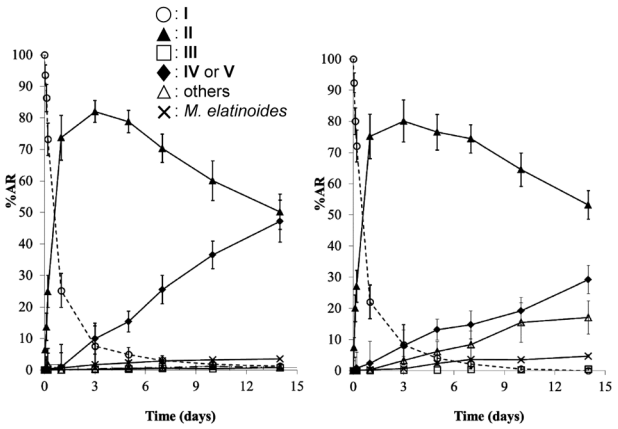

Fig. 5. ^{14}C distribution in the water exposure system with *M. elatinoides* (left: [THP-^{14}C] label, right: [PH-^{14}C] label). The error bars represent standard deviation of triplicate samples (n=3).

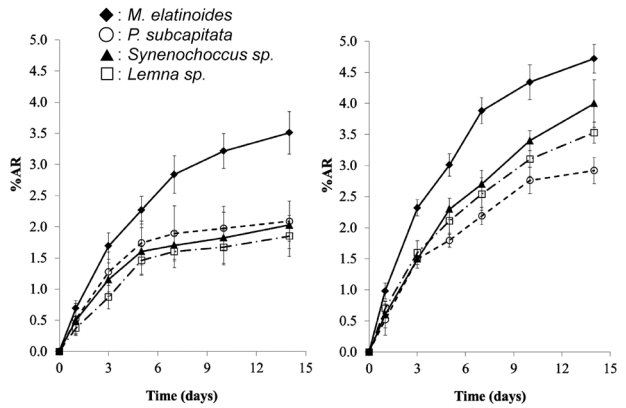

Fig. 6. ^{14}C accumulation by plants in the water exposure system ([THP-^{14}C] label). The error bars represent standard deviation of triplicate samples (n=3).

sediment particles (41.3%AR and 61.4%AR in sediment particles for [THP-^{14}C] and [PH-^{14}C] labels, respectively, at Day 14), showing a degradation product distribution and transition similar to the one observed in the water exposure. The ^{14}C root uptake by water milfoil was extremely low, not exceeding 0.9%AR for both radiolabels, and no detectable ^{14}C was transported to the shoot portion.

The behavior and metabolic pathways of **I** in aquatic plants/phytoplankton are summarized in Fig. 7. In the detoxification of organic compounds in algae and macrophytes, phase I metabolic reactions by CYP or its isozymes such as EROD and ECOD have been reported.[32–34] Similarly, phase II reactions against xenobiotics to generate glucose and GSH conjugates are known in aquatic plants/phytoplankton.[34–37] In addition to glucose and GSH conjugations, direct *N*-conjugations with organic acids are major modifications in terrestrial plants, such as: *N*-malonyl conjugations catalyzed by malonyltransferase in a stereo-selective manner or dependent on plant species[38–40]; *N*-acetylation mediated by acetyltransferase,[41] while the reaction can be proceeded by the function of symbiotic microbes[42]; and conjugations with lactic acid, alanine, and acetic acid, known as major detoxification processes for a variety of triazole derivatives.[43] As with terrestrial plants, some of these phase II conjugations have also been reported for aquatic plants/pytoplankton.[17,44] *N*-lactic acid conjugation, as well as *N*-alanine and *N*-acetic acid conjugations found in our study, has hitherto not been reported for aquatic/phytoplankton. Although further studies are necessary to conclude whether these aquatic species have the same arsenals of xenobiotic detoxification as terrestrial plants, it is likely that they have capacities comparable to those of terrestrial plants, and the metabolism pathway and degree are deemed to depend on the species.

Concluding Remarks

By these studies, fundamental information regarding each dynamic and metabolic behavior of the chemicals and the herbicide in water milfoil was successfully obtained. Similar experimental approaches are considered fully applicable for demonstrating the fate of pesticides and the results to be generated are expected to be very useful for in-depth risk assessments of the species, which can even be extended to evaluate/discuss higher-tier risks *e.g.*, biomagnification. In conducting the study, incorporating knowledge of the pesticide distribution at the water column/sediment and the simulated exposure concentration in the natural environments is essential for obtaining pragmatic data to enforce realistic risk evaluations. Due to that the fact that the metabolic reactions appearing in aquatic plants/phytoplankton in our studies were the basic detoxification methods known in terrestrial plants, their metabolic potentials are considered similar; therefor, plenty of knowledge available for terrestrials can be applied. However, terrestrial and aquatic plants/phytoplankton living in different environments would be exposed to dissimilar pesticide-derived chemicals. Specifically, a pesticide sprayed on the surface of terrestrial plants absorbs the sunlight to cause photo-excitation followed by radical-mediated isomerization/degradation; it also reacts with reactive oxygen species such as ·OH, O_3, and $^1O_2$. On the other hand, aqueous pho-

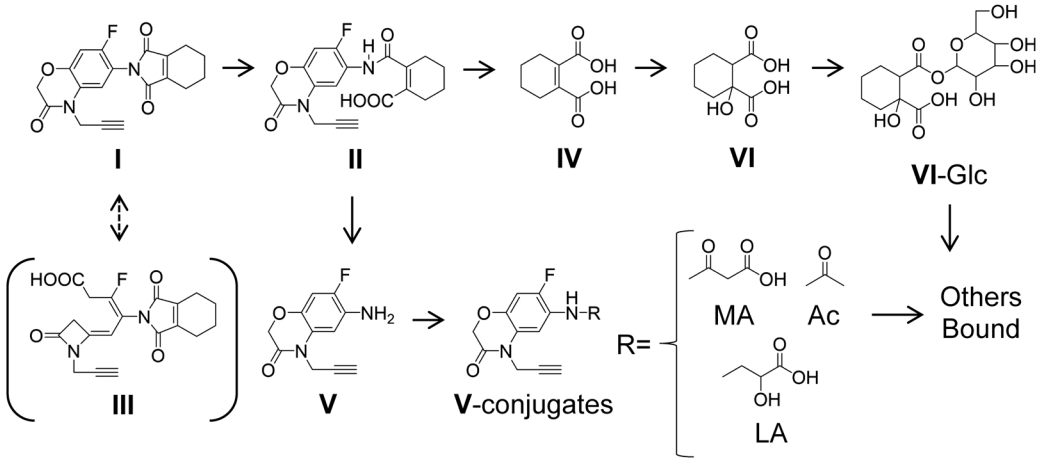

Fig. 7. Proposed metabolic pathway of flumioxazin (**I**) in aquatic plants/phytoplankton.

tolysis under different structural (free) rotation degrees and/or quantum yields of the pesticide proceed with hydrolysis, which are accompanied by enhancing/suppressing effects of dissolved or dispersed organic matters and inorganics. Besides, microbial reactions involved with each community may vary. These overall factors produce differences in the pesticide-derived exposure species and could cause large variations in the distribution and residual levels of pesticides and degradates in terrestrial and aquatic plants/phytoplankton; thus, it is essential to sufficiently understand the behavior of pesticides in each compartment and comprehensively discuss the fate of pesticide by taking realistic exposure conditions into account.

Acknowledgements

The author is greatly pleased to be chosen for this honorable award and would like to deeply thank the members of the Pesticide Science Society of Japan. These studies were made at Sumitomo Chemical Co., Ltd. I would like to express my deepest gratitude to Dr. Toshiyuki Katagi (Research Director of Bioscience Research Laboratory), Dr. Yoshitaka Tomigahara (Research Director of the Environmental Health Science Laboratory), Dr. Takuo Fujisawa (Group Manager of the Environmental Science Group) and other co-workers in Sumitomo Chemical Co., Ltd. for their scientific guidance, expertise, discussions, and warm encouragement which greatly helped me to promote the research. I would also like to show my sincere appreciation to Professor Dr. Kazuhito Itoh (Dean of The Faculty of Life and Environmental Sciences of Shimane University) for significant input and insightful comments.

References

1) M. Scheffer: "Ecology of Shallow Lakes," Chapman and Hall, New York, pp. 357 (1998).
2) L. Marion and J. M. Paillisson: *Aquat. Bot.* **73**, 249–260 (2002).
3) J. D. Madsen, P. A. Chambers, W. F. James, E. W. Koch and D. F. Weslake: *Hydrobiogia* **71**, 70–84 (2001).
4) L. Maltby, D. Arnold, G. Arts, J. Davies, F. Heimbach, C. Pickl and V. Poulsen: "Aquatic Macrophyte Risk Assessment for Pesticide," ed. by J.W. Gorsuch, CRC Press, Boca Ranton, FL, pp. 5–7 (2009).
5) A. L. Lewis: *Environ. Pollut.* **87**, 319–336 (1995).
6) M. D. J. Belgers, J. R. Van Lieverloo, T. J. L. Van der Pas and J. P. Van den Brink: *Aquat. Bot.* **86**, 260–268 (2007).
7) N. Cedergreen, C. J. Streibig and H. N. Spliid: *Ecotoxicol. Environ. Saf.* **57**, 153–161 (2004).
8) C. Turgut and A. Fomin: *Bull. Environ. Contam. Toxicol.* **69**, 601–608 (2002).
9) European Food Safety Authority (EFSA): *EFSA J.* **11**, 3290 (2013).
10) M. L. Hinman and S. J. Klaine: *Environ. Sci. Technol.* **26**, 609–613 (1992).
11) N. J. Diepens, G. H. P. Arts, A. Focks and A. A. Koelmans: *Environ. Sci. Technol.* **48**, 12344–12353 (2014).
12) A. Fritiof and M. Greger: *Chemosphere* **67**, 365–375 (2007).
13) D. Ando, T. Fujisawa and T. Katagi: *J. Pestic. Sci.* **37**, 342–346 (2012).
14) OECD: "OECD Guidelines for the Testing of Chemicals 201, Freshwater Alga and Cyanobacteria, Growth Inhibition Test" (2002).
15) OECD: "OECD Guidelines for the Testing of Chemicals 218, Sediment-Water Chironomid Toxicity Using Spiked Sediment" (2004).
16) J. P. Leahey: "Metabolism and Environmental Degradation," ed. by J.P. Leahey, Taylor & Francis, London, pp. 263–342 (1979).
17) T. Fujisawa, M. Kurosawa and T. Katagi: *J. Agric. Food Chem.* **54**, 6286–6293 (2006).
18) R. H. Shimabukuro and W. C. Walsh: "Xenobiotic metabolism in plants," eds. by D.G. Paulson, S.D. Frear and P.E. Marks, ACS Symposium Series, American Chemical Society, Washington. DC, Vol. 97, Chap. 1, pp. 3–34 (1979).
19) D. Ando, T. Fujisawa and T. Katagi: *J. Agric. Food Chem.* **63**, 5189–5195 (2015).
20) C. H. Van der Waterbeemd and B. Testa: *Adv. Drug Res.* **16**, 85–225 (1987).
21) C. Hansch and A. J. Leo: "Substituent Constant for Analysis in Chemistry and Biology," Wiley, New York, pp. 171–319 (1979).
22) F. A. P. C. Gobas, E. J. McNell, L. Lovett-Doust and G. D. Haffner: *Environ. Sci. Technol.* **25**, 924–929 (1991).
23) R. F. de Carvalho, R. H. Bromilow and R. Greenwood: *Pest Manag. Sci.* **63**, 789–797 (2007).
24) R. F. de Carvalho, R. H. Bromilow and R. Greenwood: *Pest Manag. Sci.* **63**, 798–802 (2007).
25) W. Fu, A. Franco and S. Trapp: *Environ. Toxicol. Chem.* **28**, 1372–1379 (2009).
26) D. Zhang, R. M. Gersberg, W. J. Ng and S. K. Tan: *Environ. Pollut.* **184**, 620–639 (2014).
27) C. Rendal, K. O. Kusk and S. Trapp: *Environ. Toxicol. Chem.* **30**, 2395–2406 (2011).
28) M. Modolo, L. Li, H. Pan, J. W. Blount, R. A. Dixon and X. Wang: *J. Mol. Biol.* **392**, 1292–1302 (2009).
29) J. B. Siegel, A. Zanghellini, H. M. Lovick, G. Kiss, A. R. Lambert, J. L. St. Clair, J. L. Gallaher, D. Hilvert, M. H. Gelb, B. L. Stoddard, K. N. Houk, F. E. Michael and D. Baker: *Science* **392**, 309–313 (2010).
30) D. Ando, T. Fujisawa and T. Katagi: *J. Agric. Food Chem.* **65**, 8813–8822 (2017).
31) European Food Safety Authority (EFSA): *EFSA J.* **12**, 3736 (2014).
32) F. Thies, T. Backhaus, B. Bossmann and L. H. Grimme: *Plant Physiol.* **112**, 361–370 (1996).
33) M. Torres, P. M. Barros, C. G. S. Campos, E. Pinto, S. Rajamani, T. R. Sayre and P. Colepicolo: *Ecotoxicol. Environ. Saf.* **71**, 1–15 (2008).
34) S. Pflugmacher and C. Steinberg: *J. Appl. Bot. Food Qual.* **71**, 144–146 (1997).
35) S. Pflugmacher and H. Sandermann Jr.: *Phytochemistry* **49**, 507–511 (1998).
36) S. Pflugmacher, C. Wiencke and H. Sandermann: *Mar. Environ. Res.* **48**, 23–36 (1999).
37) S. Pflugmacher, P. Schröder and H. Sandermann Jr.: *Phytochemistry* **54**, 267–273 (2000).
38) R. Winkler and H. Sandermann Jr.: *Pestic. Biochem. Physiol.* **33**, 239–248 (1989).
39) S. Lao, C. Loutre, M. Brazier, J. Coleman, D. Cole, R. Edward and F. Theodoulou: *Phytochemistry* **63**, 653–661 (2003).
40) H. Sandermann Jr., R. Schmitt, H. Eckey and T. Bauknecht: *Arch. Biochem. Biophys.* **287**, 341–350 (1991).
41) K. Ford and J. Casida: *J. Agric. Food Chem.* **56**, 10168–10175 (2008).
42) F. L. Rodrigues, J. Dairou, C. L. Diaz, M. C. Rubio, E. Sim, H. P. Spaink and J. M. Dupret: *Mol. Microbiol.* **60**, 505–512 (2006).
43) FAO: Triazole fungicide metabolites toxicology. http://www.fao.org/fileadmin/templates/agphome/documents/Pests_Pesticides/JMPE/Report08/Triazole.pdf (accessed 15 May 2020).
44) K. Mitsou, A. Koulianou, D. Lambropoulou, P. Pappas, T. Albanis and M. Lekka: *Chemosphere* **62**, 275–284 (2006).